



Unexpected Functional Divergence of Bat Influenza Virus NS1 Proteins

Turkington, H L ; Juozapaitis, M ; Tsolakos, N ; Corrales-Aguilar, E ; Schwemmler, M ; Hale, B G

Abstract: Recently, two influenza A virus (FLUAV) genomes were identified in Central and South American bats. These sequences exhibit notable divergence from classical FLUAV counterparts, and functionally, bat FLUAV glycoproteins lack canonical receptor binding and destroying activity. Nevertheless, other features that distinguish these viruses from classical FLUAVs have yet to be explored. Here, we studied the viral non-structural protein, NS1, a virulence factor that modulates host signaling to promote efficient propagation. Like all FLUAV NS1 proteins, bat FLUAV NS1s bind double-stranded RNA and act as interferon-antagonists. Unexpectedly, we found that bat FLUAV NS1s are unique in being unable to bind host p85, a regulatory subunit of the cellular metabolism-regulating enzyme, phosphoinositide 3-kinase (PI3K). Furthermore, neither bat FLUAV NS1 alone, nor infection with a chimeric bat FLUAV, efficiently activates Akt, a PI3K effector. Structure-guided mutagenesis revealed that the bat FLUAV NS1:p85 interaction can be re-engineered (in a strain-specific manner) by changing 2-4 NS1 residues (96L, 99M, 100I and 145T) thereby creating a hydrophobic patch. Notably, ameliorated p85-binding is insufficient for bat FLUAV NS1 to activate PI3K, and a chimeric bat FLUAV expressing NS1 with engineered hydrophobic patch mutations exhibits cell-type dependent, but species independent, propagation phenotypes. We hypothesize that bat FLUAV hijack of PI3K in the natural bat host has been selected against, perhaps because genes in this metabolic pathway were differentially shaped by evolution to suit unique energy-use strategies of this flying mammal. Our data expand understanding of the enigmatic functional divergence between bat FLUAVs and classical mammalian and avian FLUAVs. **IMPORTANCE** The potential for novel influenza A viruses to establish infections in humans from animals is a source of continuous concern due to possible severe outbreaks or pandemics. The recent discovery of influenza A-like viruses in bats has raised questions over whether these entities could be a threat to humans. Understanding unique properties of the newly-described bat influenza A-like viruses, such as their mechanisms to infect cells or how they manipulate host functions, is critical to assess their likelihood of causing disease. Here, we characterized the bat influenza A-like virus NS1 protein, a key virulence factor, and found unexpected functional divergence of this protein from counterparts in other influenza A viruses. Our study dissects the molecular changes required by bat influenza A-like virus NS1 to adopt classical influenza A virus properties, and suggests consequences of bat influenza A-like virus infection, potential future evolutionary trajectories, and intriguing virus-host biology in bat species.

DOI: <https://doi.org/10.1128/JVI.02097-17>

Posted at the Zurich Open Repository and Archive, University of Zurich

ZORA URL: <https://doi.org/10.5167/uzh-145423>

Journal Article

Accepted Version

Originally published at:

Turkington, H L; Juozapaitis, M; Tsolakos, N; Corrales-Aguilar, E; Schwemmle, M; Hale, B G (2018). Unexpected Functional Divergence of Bat Influenza Virus NS1 Proteins. *Journal of Virology*, 92(5):e02097-17.
DOI: <https://doi.org/10.1128/JVI.02097-17>

1 **Unexpected Functional Divergence of Bat Influenza Virus NS1 Proteins**

2

3

4 Hannah L. Turkington^a, Mindaugas Juozapaitis^{b,c}, Nikos Tsolakos^a, Eugenia Corrales-

5 Aguilar^d, Martin Schwemmle^{b,c} & Benjamin G. Hale^{a#}

6

7 Institute of Medical Virology, University of Zurich, Switzerland^a; Institute of Virology,

8 Medical Center – University of Freiburg, Germany^b; Faculty of Medicine, University of

9 Freiburg, Germany^c; Virology-CIET (Research Center for Tropical Diseases), Microbiology,

10 University of Costa Rica, San José, Costa Rica^d

11

12

13 **Running head:** An Unexpected Bat FLUAV NS1 Feature

14 [#]Address correspondence to Benjamin G. Hale, hale.ben@virology.uzh.ch

15

16

17

18 **Abstract word length:** 250

19 **Text word length:** 4,070 (excluding references and figure legends)

20

21

ABSTRACT

Recently, two influenza A virus (FLUAV) genomes were identified in Central and South American bats. These sequences exhibit notable divergence from classical FLUAV counterparts, and functionally, bat FLUAV glycoproteins lack canonical receptor binding and destroying activity. Nevertheless, other features that distinguish these viruses from classical FLUAVs have yet to be explored. Here, we studied the viral non-structural protein, NS1, a virulence factor that modulates host signaling to promote efficient propagation. Like all FLUAV NS1 proteins, bat FLUAV NS1s bind double-stranded RNA and act as interferon-antagonists. Unexpectedly, we found that bat FLUAV NS1s are unique in being unable to bind host p85 β , a regulatory subunit of the cellular metabolism-regulating enzyme, phosphoinositide 3-kinase (PI3K). Furthermore, neither bat FLUAV NS1 alone, nor infection with a chimeric bat FLUAV, efficiently activates Akt, a PI3K effector. Structure-guided mutagenesis revealed that the bat FLUAV NS1:p85 β interaction can be re-engineered (in a strain-specific manner) by changing 2-4 NS1 residues (96L, 99M, 100I and 145T) thereby creating a hydrophobic patch. Notably, ameliorated p85 β -binding is insufficient for bat FLUAV NS1 to activate PI3K, and a chimeric bat FLUAV expressing NS1 with engineered hydrophobic patch mutations exhibits cell-type dependent, but species independent, propagation phenotypes. We hypothesize that bat FLUAV hijack of PI3K in the natural bat host has been selected against, perhaps because genes in this metabolic pathway were differentially shaped by evolution to suit unique energy-use strategies of this flying mammal. Our data expand understanding of the enigmatic functional divergence between bat FLUAVs and classical mammalian and avian FLUAVs.

IMPORTANCE

48

49

50 The potential for novel influenza A viruses to establish infections in humans from animals is a
51 source of continuous concern due to possible severe outbreaks or pandemics. The recent
52 discovery of influenza A-like viruses in bats has raised questions over whether these entities
53 could be a threat to humans. Understanding unique properties of the newly-described bat
54 influenza A-like viruses, such as their mechanisms to infect cells or how they manipulate host
55 functions, is critical to assess their likelihood of causing disease. Here, we characterized the
56 bat influenza A-like virus NS1 protein, a key virulence factor, and found unexpected
57 functional divergence of this protein from counterparts in other influenza A viruses. Our study
58 dissects the molecular changes required by bat influenza A-like virus NS1 to adopt classical
59 influenza A virus properties, and suggests consequences of bat influenza A-like virus
60 infection, potential future evolutionary trajectories, and intriguing virus-host biology in bat
61 species.

62

INTRODUCTION

In 2012 and 2013, two novel influenza A virus (FLUAV) genomes were discovered by RT-PCR analysis of rectal samples from two species of Guatemalan and Peruvian fruit bats (1, 2). Due to high sequence and evolutionary divergence in multiple genomic segments, as compared with other FLUAVs, these viruses were designated the unique subtypes HL17NL10 and HL18NL11 (1-3). Functional characterization of bat FLUAVs and their encoded proteins using reverse genetic or reductionist techniques have since revealed remarkable properties of these viruses [reviewed in (3-6)]. For example, bat FLUAV surface glycoproteins lack canonical receptor binding or destroying features (7-10), and these viruses preferentially enter polarized cells at the basolateral membrane (11). Thus, bat FLUAVs appear to have evolved unique mechanisms for entering host cells that are distinct from classical mammalian and avian FLUAVs. Other features that distinguish bat FLUAVs from other FLUAVs have yet to be explored in detail.

The precise host-range and zoonotic potential of bat FLUAVs is unknown, although depending upon the experimental system used these viruses can infect cells from an array of species, including bats, humans and dogs (11-13). Reassortment of bat FLUAVs with classical FLUAVs has never been observed in experimental studies (14-16), although a cell-line derived from the bat species *Pteropus alecto* can support replication and reassortment of avian, swine and human FLUAVs (17). In addition, there is evidence that bat species can be naturally infected with classical FLUAVs: in one study 30% of Ghanaian fruit bats analyzed were seropositive for avian H9 FLUAVs (18), and the respiratory and gastro-intestinal tracts of North American little brown bats harbor receptors for both avian and mammalian FLUAVs (19). Thus, these data suggest that bats could represent an additional reservoir for FLUAVs, with the potential to provide either new gene segments or entire viruses that cross the species

89 barrier with unknown consequences. Understanding fundamental properties of the newly-
90 described bat FLUAVs, such as their mechanisms to infect cells of certain species and how
91 they modulate functions of the infected host-cell environment, will be critical to assess their
92 likelihood for causing disease in particular hosts.

93

94 We have focused on the non-structural protein, NS1, of bat FLUAVs, which shares only
95 ~50% sequence identity with other FLUAV NS1 proteins. NS1 is a multifunctional virulence
96 factor that can contribute to virus host-range and virulence (20, 21). A major role of NS1
97 during FLUAV infection is to antagonize the host innate interferon (IFN) system through
98 multiple mechanisms, some of which appear to be strain-dependent (22-31). We and others
99 have recently demonstrated that bat FLUAV NS1 proteins, like classical FLUAVs, harbor a
100 structurally- and functionally- conserved N-terminal double-stranded (ds) RNA-binding
101 domain that is critical for potent IFN-antagonism in human cells (15, 32, 33). The C-terminal
102 effector domain (ED) of bat FLUAV NS1 may play a minor role in supporting IFN-
103 antagonism *in vitro* (15), possibly by promoting NS1 oligomerization (34-37). However, a
104 striking finding is that deletion of the bat FLUAV NS1 ED has minimal impact on viral
105 pathogenesis in a mouse model as compared to deletion of this NS1 domain in a human H1N1
106 FLUAV (15). This suggests unappreciated functional differences between the EDs of bat and
107 classical FLUAVs that remain to be explored. Here, we investigated one such activity of the
108 NS1 ED: modulation of the host intracellular metabolic environment by binding the p85 β
109 regulatory subunit of phosphoinositide 3-kinase (PI3K) (38). The NS1 EDs of all classical
110 human and avian FLUAV strains tested to date bind the inter-SH2 (iSH2) domain of host
111 p85 β to activate PI3K signaling (38-42). This activation generally benefits classical FLUAV
112 replication, as viruses engineered to express NS1 proteins unable to bind p85 β are attenuated
113 for replication *in vitro* and for virulence *in vivo* (38, 43, 44). In this study, we found that bat
114 FLUAV NS1 proteins uniquely lack the ability to bind host p85 β and activate PI3K signaling.

115 We map the bat FLUAV NS1 ED residues responsible for this atypical binding phenotype,
116 and characterize the impact that artificial introduction of this property into a model bat
117 FLUAV has on virus propagation *in vitro*. Our data reveal unexpected functional divergence
118 of bat FLUAV NS1 proteins from classical FLUAV NS1 proteins, and may suggest that
119 specific metabolic conditions in the bat host *in vivo* negate any requirement for NS1 to evolve
120 to engage with host PI3K signaling in these species.

121

122

RESULTS

123

124 **Bat FLUAV NS1 proteins are unable to bind p85 β .** As part of a larger project to
125 understand the interplay between FLUAV NS1 proteins and host PI3K, we screened a panel
126 of different NS1s from various virus strains for their ability to interact with human p85 β , or
127 the related isoform, p85 α . To this end, 293T cells were co-transfected with plasmids
128 expressing FLAG-tagged human p85 α or p85 β , together with plasmids expressing V5-tagged
129 GST or NS1 proteins from representative human, swine, avian and bat strains. Soluble
130 fractions were prepared from cell lysates 48 h post-transfection, and were subjected to
131 immunoprecipitation with an antibody raised against the V5 tag. Western blot analysis of the
132 resulting precipitates revealed that NS1 proteins from human (PR8, H1N1; and Cal/09,
133 pdmH1N1), swine (Sw/Tx/98, H3N2) and avian (Nig/07, H5N1; and Sh/13, H7N9) strains
134 were all capable of interacting specifically with human p85 β , but not p85 α (**Fig. 1A**).
135 Surprisingly, NS1 proteins from bat FLUAVs (Guat/09, HL17NL10; and Peru/10,
136 HL18NL11) were unable to precipitate either p85 α or p85 β (**Fig. 1B**). This phenotype has not
137 previously been observed for a naturally-occurring FLUAV NS1 protein, but is akin to the
138 more distantly related influenza B virus (FLUBV) NS1, which is also unable to bind PI3K
139 subunits (45, 46).

140

141 **Bat FLUAV NS1 proteins do not show a species-specific interaction with p85 β .** To
142 examine if the interaction between bat FLUAV NS1 proteins and host p85 β is species-
143 specific, we generated an expression vector for bat (*Myotis lucifugus*) p85 β , and assessed its
144 co-immunoprecipitation with various NS1 proteins. While PR8/NS1 interacted with this bat
145 p85 β to an extent similar to human p85 β , neither the Guat/09 nor Peru/10 bat FLUAV NS1
146 proteins were able to precipitate bat p85 β (**Fig. 2A**). To exclude the possibility that this lack of
147 p85 β -binding was due to *M. lucifugus* not being the primary bat host species for bat FLUAVs,
148 we sought to generate expression vectors mimicking p85 β from the bat species *Sturnia lilium*
149 (in which the HL17NL10 virus genome was first discovered (1)) and *Carollia perspicillata*
150 (in which individual animals sero-positive for HL18NL11 have been identified (2)). To this
151 end, we cloned and sequenced the region encoding the p85 β iSH2 domain from tissue
152 originally derived from *S. lilium* and *C. perspicillata*. As shown in **Fig. 2B**, the human and bat
153 p85 β iSH2 domains are almost identical, with only 5 residue positions that differ. Three of
154 these differences are conserved in the bat species sequenced (E544, T547 and L550; bat
155 numbering), while two residue positions (605 and 611) differ between the *M. lucifugus* p85 β
156 iSH2 domain and the two other bat species (**Fig. 2B**). We therefore substituted these two
157 residue positions in the *M. lucifugus* p85 β for the respective residues from *C. perspicillata*
158 (A605S) or *S. lilium* (A605S/D611E), and assessed their abilities to co-precipitate with NS1.
159 However, neither bat p85 β variant interacted with the bat FLUAV NS1 proteins, while their
160 interaction with PR8/NS1 was unaffected (**Fig. 2C**). These data suggest that the bat FLUAV
161 NS1 proteins have not specifically evolved to bind bat p85 β .

162
163 **Bat FLUAV is an inefficient activator of PI3K signaling during infection.** In contrast to
164 PR8/NS1, and consistent with their inability to bind p85 β , isolated expression of the V5-
165 tagged NS1 proteins from Guat/09 or Peru/10 failed to stimulate phosphorylation of the
166 downstream effector of PI3K, Akt (**Fig. 3A**). To assess further the impact of bat FLUAV

167 infection on host PI3K signaling, we generated recombinant, chimeric bat FLUAVs
168 possessing the six complete internal gene segments of Guat/09 (variant C3; chHL17) and
169 modified HA and NA glycoprotein gene segments from PR8, where the untranslated regions
170 were replaced by the genome ends and packaging sequences of the corresponding segments of
171 Guat/09. Within these viruses, we also re-engineered the NS segment to allow expression of
172 different V5-tagged NS1 proteins (from PR8, Guat/09 or Peru/10) separated from Guat/09
173 NEP by a 2A sequence (**Fig. 3B**). Immunoprecipitations from infected cell lysates revealed
174 that endogenous p85 β could be co-precipitated with V5-PR8/NS1, but not with the V5-tagged
175 NS1 proteins derived from Guat/09 or Peru/10 (**Fig. 3C**). In addition, we observed that only
176 the chimeric bat FLUAV expressing V5-tagged PR8/NS1 efficiently lead to increased
177 phosphorylation of Akt during infection (**Figure 3D**). These infection data indicate that
178 additional bat FLUAV internal gene segment products are unable to compensate bat FLUAV
179 NS1 for either binding host p85 β or activating PI3K.

180
181 **A small number of amino acid changes can establish an interaction between bat FLUAV**
182 **NS1 and p85 β .** We analyzed the crystal structure of the PR8/NS1 ED in complex with the
183 p85 β iSH2 domain, taking into account recent mutagenesis data (**Fig. 4A**) (41, 47). Of the
184 NS1 residues present at this interface, 6 were selected for substitution analysis in the bat
185 FLUAV NS1 proteins based on their divergence from residues in NS1 proteins with the
186 ability to bind p85 β (**Figs. 4A and 4B**). Single amino acid substitutions at these 6 ED residues
187 in Guat/09 NS1 (Q96L, T99M, I100S, R145T, N163S and S166P; Guat/09 NS1 numbering),
188 did not result in the establishment of human p85 β binding (**Fig. 4C**). However, combining the
189 amino acid substitutions Q96L and T99M resulted in partial p85 β binding (**Fig. 4D**). The
190 interaction between Guat/09 NS1 and human p85 β could be enhanced further when the
191 additional R145T substitution was introduced (**Fig. 4D**). Substitutions at other positions
192 (particularly I100S) proved to be disruptive to the interaction (**Fig. 4D**). From these data, we

infer that creation of a hydrophobic patch around positions 96, 99 and 100 in the Guat/09 NS1 ED is essential for determining the interaction with p85 β . Largely similar, but distinct, results were obtained for substitution analysis of the Peru/10 NS1 protein: single amino acid substitution of V96L, T99M or R145T, as well as double substitution of V96L and T99M, did not establish an interaction with human p85 β (**Figs. 5A and 5B**). In fact, only when N100I was combined with double substitution of V96L and T99M could some weak p85 β binding be observed, which was strongly enhanced by R145T (**Fig. 5B**). Notably, mutant Guat/09 and Peru/10 NS1 constructs generated to possess optimal p85 β binding also exhibited the ability to interact with bat p85 β (**Fig. 5C**).

A chimeric bat FLUAV expressing an engineered p85 β -binding NS1 protein exhibits cell-type dependent, but species-independent, propagation phenotypes. Using reverse genetics, we generated chimeric bat FLUAVs as before (chHL17), but possessing authentic Guat/09 NS segments expressing either wild-type NS1 (WT) or NS1-Q96L/T99M (2x), which possesses p85 β -binding ability with a minimal number of substitutions. Strikingly, we observed that chHL17-2x exhibited an altered plaque phenotype and markedly enhanced propagation capability (>100-fold higher peak titers) in canine MDCK cells (**Figs. 6A and 6B**). Enhanced propagation of the chHL17-2x virus was also observed, to a lesser extent, in human HAP-1 cells (**Fig. 6C**). However, such a phenotype was not found in other cell-types: the chHL17-2x virus exhibited slower replication kinetics in human A549 cells, and a subtle attenuation in bat EidNi/41 cells (**Figs. 6D and 6E**). These data indicate that the Q96L/T99M substitutions in NS1 impact tissue-culture replication of the chimeric bat FLUAV in a cell-type dependent, but species-independent, manner.

Role of p85 β and PI3K activation in the phenotype of a chimeric bat FLUAV expressing NS1-Q96L/T99M. We hypothesized that the engineered binding of Guat/09 NS1-

219 Q96L/T99M to p85 β , and potential activation of PI3K signaling, was responsible for
220 modulating propagation of the chHL17-2x virus. However, similar to expression of the wild-
221 type V5-tagged NS1 protein from Guat/09, expression of V5-Guat/09 NS1-Q96L/T99M
222 failed to stimulate Akt phosphorylation (**Fig. 7A**), an observation supporting previous data
223 that other NS1 determinants beyond efficient p85 β binding can critically impact PI3K
224 activation (41, 43, 48). In addition, we assessed propagation of the chHL17-2x virus in human
225 HAP-1 cells that had been genetically-engineered to lack p85 β expression (**Fig. 7B**). Notably,
226 the chHL17-2x virus also exhibited slightly enhanced propagation in this p85 β knock-out
227 HAP-1 cell-line (**Fig. 7C**), which was similar to the enhancement previously observed in
228 wild-type HAP-1 cells (**Figs. 6C and 7D**). Overall, these data suggest that, while the
229 Q96L/T99M substitutions in Guat/09 NS1 permit host p85 β -binding, they are not sufficient
230 for this NS1 to activate host PI3K signaling. Furthermore, these NS1 substitutions may
231 impact propagation of the chimeric bat FLUAV, at least in some host substrates, in a
232 p85 β /PI3K-independent manner.

233

234 DISCUSSION

235

236 Functional characterization of proteins encoded by the novel bat FLUAV sequences has so far
237 revealed some remarkable properties, most notably that the HA-like protein does not bind
238 canonical FLUAV sialic acid receptors, and the NA-like protein lacks neuraminidase activity
239 (7-10). Herein, we describe an additional feature of classical mammalian and avian FLUAVs
240 that is missing in their bat-derived counterparts: the multifunctional bat FLUAV NS1
241 virulence factor is unable to bind host p85 β or activate PI3K signaling. This property seems
242 important for the efficient replication of many classical FLUAV strains in tissue-culture and
243 *in vivo* (38, 43, 44, 47). Using a structure-guided approach, we found that p85 β -binding could
244 be engineered into the bat FLUAV NS1 proteins with a minimum of only 2 amino-acid

245 substitutions (Q96L/T99M), and that a chimeric bat FLUAV expressing NS1 with these
246 substitutions had improved propagation kinetics in some tissue-culture systems (canine
247 MDCK and human HAP-1), but a seemingly attenuated phenotype in others (human A549
248 and bat EidNi/41). Notably, this disparate impact did not correlate with host-species, as two
249 different human cell-lines were identified in which the outcome of infection was opposite.
250 Therefore, cell-type (and thus unknown differential gene/protein expression profiles or
251 polymorphisms) likely determine the phenotypic result. Interestingly, the propagation
252 phenotype in human HAP-1 cells of the chimeric bat FLUAV expressing NS1-Q96L/T99M
253 was not diminished in an isogenic cell-line completely lacking p85 β expression, suggesting
254 that the amino-acid substitutions used to permit p85 β -binding by NS1 also modify an
255 additional property of this multifunctional viral protein that has yet to be identified. This will
256 certainly be an interesting area to explore in the future, and may impact our understanding of
257 other classical influenza A viruses and the biological consequences of certain NS1
258 polymorphisms that they harbor. Such observations will also have implications when
259 assessing potential virological consequences of the p85 β -binding property arising naturally in
260 bat FLUAVs.

261

262 Engineering p85 β -binding into the bat FLUAV NS1 protein did not result in detectable
263 activation of PI3K signaling, indicating that additional regions of NS1 are essential for this
264 function. Indeed, while p85 β -binding is necessary for NS1-mediated PI3K activation (38), our
265 data suggest that it is not sufficient, an observation consistent with previous work (41, 48).
266 Glutamic acid residues at human FLUAV NS1 positions 96 and 97 (equivalent to bat FLUAV
267 NS1 positions 97 and 98) do not interact directly with p85 β , but have been proposed to form
268 part of an 'activating interface' with the p110 catalytic subunit of the p85 β -containing PI3K
269 heterodimer (41). Although these are the only non-p85 β -interface residues so far implicated in
270 NS1-activated PI3K signaling, they are conserved in the bat FLUAV NS1 proteins, meaning

271 that another unidentified region of classical FLUAV NS1 proteins must be responsible for
272 ensuring PI3K activation. Experiments to uncover this specific region are currently underway,
273 but it is therefore apparent that more than the 2-4 amino-acid substitutions required for p85 β -
274 binding would be necessary to allow bat FLUAV NS1 proteins to fully acquire PI3K
275 activation potential, constituting a relatively high genetic barrier to natural evolution of this
276 property.

277

278 Our studies suggest that interactions between NS1 and p85 β are not species-specific: bat
279 FLUAV NS1 proteins do not bind bat p85 β . Thus, an open question is why bat FLUAVs have
280 not retained (or evolved) this property like classical mammalian and avian FLUAVs? One
281 hypothesis for this observation is that the natural host environment encountered *in vivo* by bat
282 FLUAVs is in a particular metabolic state such that viral augmentation of PI3K signaling
283 would not alter host physiology. Indeed, recent genome sequencing and analysis studies have
284 begun to uncover major differences between bats and other species, and have linked
285 specialized adaptations of bats (e.g. flying ability, longevity, hibernation and echolocation)
286 with specific adaptive evolution of energy metabolism genes. Such genes include those
287 involved in oxidative phosphorylation (49), insulin/growth factor receptor signaling (50), and
288 DNA damage repair and apoptosis (51), pathways otherwise known to be regulated by PI3K
289 in many mammalian systems (52, 53). Possible links between positive selection in bat
290 metabolic genes and decreased sensitivity to PI3K-mediated regulation need to be validated
291 experimentally, but could account for bat FLUAV NS1 proteins adopting a different
292 evolutionary path to those from their classical FLUAV counterparts in other species. Such
293 functional divergence of bat FLUAV NS1 proteins underscores the uniqueness of these
294 newly-discovered viruses, and suggests new and intriguing virus-host interaction biology in
295 bat species that remains to be explored.

MATERIALS AND METHODS

296

297

298 **Cells.** MDCK (canine), 293T (human), A549 (human), 1321N1 (human), EidNi/41 (bat;
299 *Eidolon helvum*) (54) and CarperAEC.B-3 (bat; *Carollia perspicillata*) (55) cells were
300 cultured in DMEM supplemented with 10% fetal bovine serum (FBS), 100 units/mL
301 penicillin and 100 µg/mL streptomycin (Gibco Life Technologies). HAP-1 cells (Horizon
302 Discovery, Austria) were cultured in IMDM supplemented with the same additives as well as
303 200µM GlutaMaxTM (Gibco Life Technologies). The HAP-1 cell-line engineered by
304 CRISPR/Cas9 to have a 2bp deletion in the *PIK3R2* gene (encoding p85β) was purchased
305 from Horizon Discovery, Austria (catalogue ID: HZGHC003292c006). All cells were
306 maintained at 37°C with 5% CO₂.

307

308 **Expression plasmids.** The NS1 cDNA sequences from A/Swine/Texas/4199-2/98 (Sw/Tx/98,
309 H3N2), A/Nigeria/OG10/2007 (Nig/07, H5N1), A/Shanghai/2/S1078/2013 (Sh/13, H7N9),
310 A/little yellow shouldered bat/Guatemala/153/2009 (Guat/09, HL17NL10) and A/flat-faced
311 bat/Peru/033/2010 (Peru/10, HL18NL11) were PCR amplified from existing plasmids and
312 ligated in-frame with an N-terminal V5-tag into modified pLVX-IRES-ZsGreen1 or pLVX-
313 IRES-Puro plasmids (Clontech, USA). Similar plasmids expressing glutathione S-transferase
314 (GST) and NS1 sequences from A/Puerto Rico/8/1934 (PR8, H1N1) or A/California/04/09
315 (Cal09, pdmH1N1) have been described previously (47). All NS1-encoding cDNAs contained
316 silent mutations in the splice acceptor site to prevent expression of NEP. Human p85α and
317 p85β cDNA sequences from existing plasmids, or the bat (*Myotis lucifugus*) p85β cDNA
318 sequence generated using the GeneArt gene synthesis service (Thermo Fisher), were PCR
319 amplified and ligated in-frame into p3xFLAG-CMV-7.1 (Sigma-Aldrich) so as to express
320 with N-terminal FLAG tags. Two step overlap PCR or Quikchange II XL (Agilent
321 Technologies, Switzerland) was used to introduce site-directed mutations into cDNAs as

322 required. The identity of all constructs was confirmed by sequencing. All plasmid
323 transfections were performed using Fugene HD (Promega) at 1:3 DNA:transfection reagent
324 ratio. As appropriate, generation of lentiviruses and production of stable cell-lines
325 constitutively expressing proteins of interest were carried out as previously described (38).

326

327 **Virus reverse genetics.** Plasmids for rescuing chimeric, recombinant HL17NL10 virus
328 (variant C3: PA-S550R and M2-N31S/T70A) were described previously (14). pHW2000
329 rescue plasmids comprising the genome ends and packaging sequences of HL17NL10 and the
330 PR8 HA or NA glycoprotein ORFs were generated as described (15). Briefly, the untranslated
331 regions of PR8 HA and NA genome segments were replaced with the genome ends and
332 packaging sequences of the corresponding segments of HL17NL10 by assembly PCR.
333 Plasmids encoding NS segments where NS1 and NEP ORFs were separated by the 2A self-
334 cleaving peptide of porcine teschovirus (allowing N-terminal V5-tagging of NS1) were
335 generated by assembly PCR according to a previous strategy (56). All generated NS chimeras
336 contained silent mutations in the splice acceptor and donor sites of the ORFs to prevent
337 aberrant splicing, and duplicated genome packaging sequences were introduced flanking the
338 NS1 ORF to avoid packaging defects. Quikchange II XL (Agilent Technologies, Switzerland)
339 was used to introduce site-directed mutations into cDNAs as required. For rescues, 6×10^5
340 293T cells were seeded in 6-well plates and co-transfected 24h later with the 8 pDZ- or
341 pHW2000- based plasmids. Twenty-four hours post-transfection, cells were washed once in
342 sterile phosphate-buffered saline (PBS) and 3×10^5 MDCK cells were added in DMEM
343 supplemented with $1 \mu\text{g/mL}$ tosylsulfonyl phenylalanyl chloromethyl ketone (TPCK)-treated
344 trypsin (Sigma-Aldrich, MO). Forty-eight hours later, supernatants were harvested, viruses
345 plaque-purified, and virus stocks grown and titrated using standard methods in MDCK cells.
346 RNA was extracted from stock aliquots using the ReliaPrepTM RNA Cell Miniprep System

347 (Promega), and the NS genomic segments of each virus were fully sequenced after segment-
348 specific reverse transcription-PCR (RT-PCR) to ensure absence of undesired mutations.

349

350 **Virus infections.** For all infections, viruses were diluted in PBS supplemented with 100
351 units/mL penicillin, 100 µg/mL streptomycin (Gibco Life Technologies), 0.3% BSA (Sigma-
352 Aldrich) and 1 mM $\text{Ca}^{2+}/\text{Mg}^{2+}$. For HAP-1 cells, cells were seeded onto poly-L-lysine
353 (Sigma-Aldrich) coated plates and infected 24 h later at the indicated multiplicity of infection
354 (MOI) for 1 h at 37°C. Following infection, cells were washed three times and overlaid with
355 FBS-free IMDM. For serum-starvation experiments, cells were washed 3 times with FBS-free
356 IMDM and incubated overnight prior to infection.

357

358 For virus growth analyses, cells in 12-well plates were infected with the indicated virus at the
359 indicated MOI. Following infection at 37°C for 1 h, cells were washed three times with PBS,
360 and overlaid with DMEM supplemented with 100 units/mL penicillin, 100 µg/mL
361 streptomycin (Gibco Life Technologies) and 0.5 µg/mL TPCK-treated trypsin (Sigma-
362 Aldrich). Supernatant samples were harvested at the indicated timepoints and stored at -80°C
363 prior to titration by standard plaque assay.

364

365 **Sequencing of p85β (PIK3R2) iSH2 domains from bat species.** Bats (*S. lilium*) were
366 captured with mist nets. Specimens were collected and processed after approval of the
367 Institutional Committee of Care and Use of Animals (IACUC) of the University of Costa Rica
368 (CICUA-36-13) according to national guidelines for animal caring described in the Costa
369 Rica National Law for Animal Welfare 7451. For sequencing, 2.5×10^5 CarperAEC.B-3 cells
370 seeded in 12-well plates, or an equivalent amount of cellular material from *S. lilium*, were
371 lysed, and RNA extracted, using the ReliaPrepTM RNA Cell Miniprep System (Promega). RT-

372 PCR products were generated, and directly sequenced, using specific primers annealing to
373 conserved regions of *PIK3R2* flanking the sequence encoding the p85 β iSH2 domain.

374

375 **Immunoprecipitations.** Transfected (2 μ g total DNA, 48 h in 293T) or infected (MOI 5
376 PFU/cell, 8 h in HAP-1) cells in 25cm² flasks or 6-well plates were lysed on ice in 1mL of
377 20mM Tris-HCl (pH 7.8), 5mM EDTA, 0.5% (v/v) NP40, and 650mM NaCl, supplemented
378 with a cOmpleteTM mini protease inhibitor tablet (Roche, Switzerland). Lysates were clarified
379 using a 29G (0.33mm) needle and centrifugation at 13,000 rpm for 40 mins at 4°C. Soluble
380 fractions were then incubated with 1 μ g of anti-V5 antibody (Bio-Rad) for 2 hours at 4°C
381 prior to further incubation overnight at 4°C with 12.5 μ L protein G sepharose beads (Sigma-
382 Aldrich). Following extensive washing, remaining proteins were dissociated from the beads
383 using urea disruption buffer (6M urea, 1M β -mercaptoethanol, 4% SDS) and heating at 95°C
384 for 10 min. Samples were stored at -20°C until analysis by SDS-PAGE and western blotting.

385

386 **Akt phosphorylation assays.** 1321N1 cells stably expressing the indicated V5-tagged protein
387 were seeded into 12-well plates and serum-starved the following day for 1 h. Cell lysates
388 were harvested in urea disruption buffer and stored at -20°C until analysis by SDS-PAGE and
389 western blotting.

390

391 **SDS-PAGE and western blotting.** Samples were sonicated to shear nucleic acids and then
392 boiled for 5 min. Polypeptides were resolved by SDS-PAGE on NuPAGE 4-12% Bis-Tris
393 protein gels (ThermoFisher), followed by transfer to nitrocellulose membranes (GE
394 Healthcare Life Sciences). Proteins were detected by western blotting using the following
395 primary antibodies: mouse anti-V5 (Bio-Rad, MCA1360); mouse anti-FLAG (Sigma-Aldrich,
396 #F3165); mouse anti-p85 β (T15; AbD Serotech, MCA1170G); rabbit anti-actin (Sigma-
397 Aldrich, #A2103); rabbit anti-Akt (Cell Signaling Technology, #4691); rabbit anti-pAkt

398 (S473) (Cell Signaling Technology, #4060); rabbit anti-NS1 (1-73) (57) (kindly provided by
399 Adolfo García-Sastre, Icahn School of Medicine at Mount Sinai, New York, USA); and rabbit
400 anti-NP (kindly provided by Silke Stertz, University of Zurich, Switzerland). Secondary
401 antibodies were fluorochrome-conjugated: anti-mouse (ThermoFisher Scientific, #SA5-
402 10176) and anti-rabbit (ThermoFisher Scientific, #SA5-10036). A LI-COR Odyssey Fc
403 scanner was used for detection.

404

405 **Structural analyses.** Structural representations were visualized using the appropriate PDB
406 file and PyMOL (58).

407

408 **FUNDING INFORMATION**

409

410 This work was supported by the Swiss National Science Foundation (grant 31003A_159993
411 to BGH), a Forschungskredit of the University of Zurich (grant FK-16-030 to HLT), and by
412 the Deutsche Forschungsgemeinschaft (SCHW 632/17-1 to MS). The funders had no role in
413 study design, data collection, data interpretation, or the decision to submit the work for
414 publication.

415

416 **ACKNOWLEDGEMENTS**

417

418 We thank Silke Stertz and Antonio M. Lopes (University of Zurich, Switzerland), Adolfo
419 García-Sastre (Icahn School of Medicine at Mount Sinai, USA) and Marcel Müller
420 (University of Bonn, Germany) for sharing material/reagents.

421

FIGURE LEGENDS

422

423

424 **Figure 1. Strain-specific interaction of FLUAV NS1 proteins with human p85 β .** 293T
425 cells were co-transfected for 48 h with plasmids expressing the indicated V5-tagged NS1
426 protein (or GST) and FLAG-tagged human p85 α or p85 β . Following cell lysis, clarification
427 and anti-V5 immunoprecipitation, soluble (input) and pull-down (IP: α -V5) fractions were
428 analyzed by SDS-PAGE and western blot. (A) Interaction studies of human (PR8, Cal/09),
429 swine (Sw/Tx/98) and avian (Nig/07, Sh/13) FLUAV NS1 proteins. (B) Interaction studies of
430 bat (Guat/09, Peru/10) FLUAV NS1 proteins. Data are representative of 3 independent
431 experiments.

432

433 **Figure 2. Bat FLUAV NS1 proteins do not show a species-specific interaction with p85 β .**

434 (A) 293T cells were co-transfected for 48 h with plasmids expressing the indicated V5-tagged
435 NS1 protein (or GST) and FLAG-tagged human (*Homo sapiens*, *H.s.*) or bat (*Myotis*
436 *lucifugus*, *M.l.*) p85 β . Following cell lysis, clarification and anti-V5 immunoprecipitation,
437 soluble (input) and pull-down (IP: α -V5) fractions were analyzed by SDS-PAGE and western
438 blot. (B) Sequence alignment of iSH2 domains from human and bat p85 β . Human (*H.*
439 *sapiens*), little yellow shouldered bat (*S. lilium*), little brown bat (*M. lucifugus*) and Seba's
440 short-tailed bat (*C. perspicillata*) p85 β iSH2 domain amino acid sequences (residues 496-614)
441 were aligned. Human/bat differences are highlighted with boxes, shading indicates residues
442 differing between bat species. (C) Experiment performed as in (A), except using the indicated
443 bat p85 β mutants. For (A) and (C), data are representative of 3 independent experiments.

444

445 **Figure 3. Bat FLUAV is an inefficient activator of PI3K signaling during infection.** (A)

446 Serum-starved 1321N1 cells stably expressing the indicated V5-tagged proteins were lysed,
447 and levels of the indicated proteins were analyzed by SDS-PAGE and western blot. (B)

448 Schematic representation of mRNAs generated by wild-type (*upper*) or engineered (*lower*)
449 NS segments. SD, splice donor; SA, splice acceptor; 2A, 2A sequence from porcine
450 teschovirus. (C) HAP-1 cells were infected for 8 h with chHL17 viruses expressing the
451 indicated V5-tagged NS1 proteins at a MOI of 5 PFU/cell. Following cell lysis, clarification
452 and anti-V5 immunoprecipitation, soluble (input) and pull-down (IP: α -V5) fractions were
453 analyzed by SDS-PAGE and western blot. (D) Serum-starved HAP-1 cells were infected with
454 chHL17 viruses expressing the indicated V5-tagged NS1 proteins at a MOI of 5 PFU/cell.
455 Cells were lysed at 3, 6 and 9 hours post-infection and levels of the indicated proteins were
456 analyzed by SDS-PAGE and western blot. For (A), (C) and (D), data are representative of at
457 least 2 independent experiments.

458

459 **Figure 4. Engineering the bat FLUAV (Guat/09) NS1 protein to bind p85 β .** (A) Crystal
460 structure of the PR8/NS1 ED in complex with part of the p85 β iSH2 domain. The NS1 ED is
461 shown in gray, with p85 β contact residues highlighted in yellow. The p85 β iSH2 domain is
462 colored blue. The six NS1 amino acid residues chosen for mutagenesis studies (see B,
463 Guat/09 numbering) are highlighted in red. Figure generated using PyMOL with PDB ID:
464 3L4Q. (B) Comparison of key NS1 ED residues between human (PR8, Cal09), swine
465 (Sw/Tx/98), avian (Nig/07, Sh/13) and bat (Guat/09, Peru/10) NS1 proteins. [#]Guat/09
466 numbering. (C-D) 293T cells were co-transfected for 48 h with plasmids expressing the
467 indicated V5-tagged NS1 protein (or GST) and FLAG-tagged human p85 β . Following cell
468 lysis, clarification and anti-V5 immunoprecipitation, soluble (input) and pull-down (IP: α -V5)
469 fractions were analyzed by SDS-PAGE and western blot. Data are representative of at least 2
470 independent experiments.

471

472 **Figure 5. Engineering the bat FLUAV (Peru/10) NS1 protein to bind p85 β .** (A-B) 293T
473 cells were co-transfected for 48 h with plasmids expressing the indicated V5-tagged NS1

474 protein (or GST) and FLAG-tagged human p85 β . Following cell lysis, clarification and anti-
475 V5 immunoprecipitation, soluble (input) and pull-down (IP: α -V5) fractions were analyzed by
476 SDS-PAGE and western blot. (C) Experiment performed as in (A), except using the indicated
477 bat p85 β mutants. Guat/09 3x = Q96L/T99M/R145T; Peru/10 4x =
478 V96L/T99M/N100I/R145T. For all panels, data are representative of at least 2 independent
479 experiments.

480
481 **Figure 6. Characterization of a chimeric bat FLUAV expressing an engineered p85 β -**
482 **binding NS1 protein.** (A) Plaque phenotype and (B) multicycle growth analysis of chHL17-
483 WT and chHL17-2x viruses in MDCK cells. (C-E) Multicycle growth analysis of chHL17-
484 WT and chHL17-2x viruses in HAP-1 (C), A549 (D) and EidNi/41 (E) cells. For all growth
485 curves, data represent mean values from 3 independent experiments (\pm SD). Significance was
486 calculated using the Student's t-test comparing chHL17-WT and chHL17-2x virus titers at each
487 time point (** $p < 0.01$, * $p < 0.05$).

488
489 **Figure 7. Role of p85 β and PI3K activation in the phenotype of a chimeric bat FLUAV**
490 **expressing NS1-Q96L/T99M.** (A) Serum-starved 1321N1 cells stably expressing the
491 indicated V5-tagged proteins were lysed, and levels of the indicated proteins were analyzed
492 by SDS-PAGE and western blot. (B) Western blot analysis of wild-type or *PIK3R2* (p85 β)
493 knock-out HAP-1 cells. For (A) and (B), data are representative of at least 2 independent
494 experiments. (C) Multicycle growth analysis of chHL17-WT and chHL17-2x viruses in
495 *PIK3R2* (p85 β) knock-out HAP-1 cells. Data represent mean values from 3 independent
496 experiments (\pm SD). (D) Ratios of chHL17-2x to chHL17-WT propagation titers (represented
497 as area under the curve (AUC) values) in wild-type and *PIK3R2* (p85 β) knock-out HAP-1
498 cells (original data from Figs. 6C and 7C). For (C) and (D), significance was calculated using

499 the Student's t-test comparing chHL17-WT and chHL17-2x virus titers at each time point (*
500 $p < 0.05$), or AUC ratios in each cell-line (ns, non significant).

501

REFERENCES

- 502 1. **Tong S, Li Y, Rivaller P, Conrardy C, Castillo DA, Chen LM, Recuenco S,**
503 **Ellison JA, Davis CT, York IA, Turmelle AS, Moran D, Rogers S, Shi M, Tao Y,**
504 **Weil MR, Tang K, Rowe LA, Sammons S, Xu X, Frace M, Lindblade KA, Cox**
505 **NJ, Anderson LJ, Rupprecht CE, Donis RO.** 2012. A distinct lineage of influenza
506 A virus from bats. *Proc Natl Acad Sci U S A* **109**:4269-4274.
- 507 2. **Tong S, Zhu X, Li Y, Shi M, Zhang J, Bourgeois M, Yang H, Chen X, Recuenco**
508 **S, Gomez J, Chen LM, Johnson A, Tao Y, Dreyfus C, Yu W, McBride R, Carney**
509 **PJ, Gilbert AT, Chang J, Guo Z, Davis CT, Paulson JC, Stevens J, Rupprecht**
510 **CE, Holmes EC, Wilson IA, Donis RO.** 2013. New world bats harbor diverse
511 influenza A viruses. *PLoS Pathog* **9**:e1003657.
- 512 3. **Ma W, Garcia-Sastre A, Schwemmle M.** 2015. Expected and Unexpected Features
513 of the Newly Discovered Bat Influenza A-like Viruses. *PLoS Pathog* **11**:e1004819.
- 514 4. **Brunotte L, Beer M, Horie M, Schwemmle M.** 2016. Chiropteran influenza viruses:
515 flu from bats or a relic from the past? *Curr Opin Virol* **16**:114-119.
- 516 5. **Wu Y, Wu Y, Tefsen B, Shi Y, Gao GF.** 2014. Bat-derived influenza-like viruses
517 H17N10 and H18N11. *Trends Microbiol* **22**:183-191.
- 518 6. **Cimini K, Thamamongood T, Zimmer G, Schwemmle M.** 2017. Novel insights
519 into bat influenza A viruses. *J Gen Virol* **98**:2393-2400.
- 520 7. **Li Q, Sun X, Li Z, Liu Y, Vavricka CJ, Qi J, Gao GF.** 2012. Structural and
521 functional characterization of neuraminidase-like molecule N10 derived from bat
522 influenza A virus. *Proc Natl Acad Sci U S A* **109**:18897-18902.
- 523 8. **Sun X, Shi Y, Lu X, He J, Gao F, Yan J, Qi J, Gao GF.** 2013. Bat-derived influenza
524 hemagglutinin H17 does not bind canonical avian or human receptors and most likely
525 uses a unique entry mechanism. *Cell Rep* **3**:769-778.
- 526 9. **Zhu X, Yang H, Guo Z, Yu W, Carney PJ, Li Y, Chen LM, Paulson JC, Donis**
527 **RO, Tong S, Stevens J, Wilson IA.** 2012. Crystal structures of two subtype N10
528 neuraminidase-like proteins from bat influenza A viruses reveal a diverged putative
529 active site. *Proc Natl Acad Sci U S A* **109**:18903-18908.
- 530 10. **Zhu X, Yu W, McBride R, Li Y, Chen LM, Donis RO, Tong S, Paulson JC,**
531 **Wilson IA.** 2013. Hemagglutinin homologue from H17N10 bat influenza virus
532 exhibits divergent receptor-binding and pH-dependent fusion activities. *Proc Natl*
533 *Acad Sci U S A* **110**:1458-1463.
- 534 11. **Moreira EA, Locher S, Kolesnikova L, Bolte H, Aydillo T, Garcia-Sastre A,**
535 **Schwemmle M, Zimmer G.** 2016. Synthetically derived bat influenza A-like viruses
536 reveal a cell type- but not species-specific tropism. *Proc Natl Acad Sci U S A*
537 doi:10.1073/pnas.1608821113.

- 538 12. **Hoffmann M, Kruger N, Zmora P, Wrensch F, Herrler G, Pohlmann S.** 2016. The
539 Hemagglutinin of Bat-Associated Influenza Viruses Is Activated by TMPRSS2 for
540 pH-Dependent Entry into Bat but Not Human Cells. *PLoS One* **11**:e0152134.
- 541 13. **Maruyama J, Nao N, Miyamoto H, Maeda K, Ogawa H, Yoshida R, Igarashi M,**
542 **Takada A.** 2016. Characterization of the glycoproteins of bat-derived influenza
543 viruses. *Virology* **488**:43-50.
- 544 14. **Juozapaitis M, Aguiar Moreira E, Mena I, Giese S, Riegger D, Pohlmann A,**
545 **Hoper D, Zimmer G, Beer M, Garcia-Sastre A, Schwemmle M.** 2014. An
546 infectious bat-derived chimeric influenza virus harbouring the entry machinery of an
547 influenza A virus. *Nat Commun* **5**:4448.
- 548 15. **Zhou B, Ma J, Liu Q, Bawa B, Wang W, Shabman RS, Duff M, Lee J, Lang Y,**
549 **Cao N, Nagy A, Lin X, Stockwell TB, Richt JA, Wentworth DE, Ma W.** 2014.
550 Characterization of uncultivable bat influenza virus using a replicative synthetic virus.
551 *PLoS Pathog* **10**:e1004420.
- 552 16. **Yang J, Lee J, Ma J, Lang Y, Nietfeld J, Li Y, Duff M, Li Y, Yang Y, Liu H,**
553 **Zhou B, Wentworth DE, Richt JA, Li Z, Ma W.** 2017. Pathogenicity of modified
554 bat influenza virus with different M genes and its reassortment potential with swine
555 influenza A virus. *J Gen Virol* **98**:577-584.
- 556 17. **Dlugolenski D, Jones L, Tompkins SM, Crameri G, Wang LF, Tripp RA.** 2013.
557 Bat cells from *Pteropus alecto* are susceptible to influenza A virus infection and
558 reassortment. *Influenza and Other Respiratory Viruses* **7**:900-903.
- 559 18. **Freidl GS, Binger T, Muller MA, de Bruin E, van Beek J, Corman VM, Rasche**
560 **A, Drexler JF, Sylverken A, Oppong SK, Adu-Sarkodie Y, Tschapka M,**
561 **Cottontail VM, Drosten C, Koopmans M.** 2015. Serological evidence of influenza A
562 viruses in frugivorous bats from Africa. *PLoS One* **10**:e0127035.
- 563 19. **Chothe SK, Bhushan G, Nissly RH, Yeh YT, Brown J, Turner G, Fisher J, Sewall**
564 **BJ, Reeder DM, Terrones M, Jayarao BM, Kuchipudi SV.** 2017. Avian and human
565 influenza virus compatible sialic acid receptors in little brown bats. *Sci Rep* **7**:660.
- 566 20. **Noronha JM, Liu M, Squires RB, Pickett BE, Hale BG, Air GM, Galloway SE,**
567 **Takimoto T, Schmolke M, Hunt V, Klem E, Garcia-Sastre A, McGee M,**
568 **Scheuermann RH.** 2012. Influenza virus sequence feature variant type analysis:
569 evidence of a role for NS1 in influenza virus host range restriction. *J Virol* **86**:5857-
570 5866.
- 571 21. **Hale BG.** 2014. Conformational plasticity of the influenza A virus NS1 protein. *J Gen*
572 *Virol* **95**:2099-2105.
- 573 22. **Krug RM.** 2015. Functions of the influenza A virus NS1 protein in antiviral defense.
574 *Curr Opin Virol* **12**:1-6.
- 575 23. **Rajsbaum R, Albrecht RA, Wang MK, Maharaj NP, Versteeg GA, Nistal-Villan**
576 **E, Garcia-Sastre A, Gack MU.** 2012. Species-specific inhibition of RIG-I

- ubiquitination and IFN induction by the influenza A virus NS1 protein. *PLoS Pathog* **8**:e1003059.
24. **Ayllon J, Domingues P, Rajsbaum R, Miorin L, Schmolke M, Hale BG, Garcia-Sastre A.** 2014. A Single Amino Acid Substitution in the Novel H7N9 Influenza A Virus NS1 Protein Increases CPSF30 Binding and Virulence. *J Virol* **88**:12146-12151.
25. **Hale BG, Steel J, Medina RA, Manicassamy B, Ye J, Hickman D, Hai R, Schmolke M, Lowen AC, Perez DR, Garcia-Sastre A.** 2010. Inefficient control of host gene expression by the 2009 pandemic H1N1 influenza A virus NS1 protein. *J Virol* **84**:6909-6922.
26. **Kochs G, Garcia-Sastre A, Martinez-Sobrido L.** 2007. Multiple anti-interferon actions of the influenza A virus NS1 protein. *J Virol* **81**:7011-7021.
27. **Twu KY, Kuo RL, Marklund J, Krug RM.** 2007. The H5N1 influenza virus NS genes selected after 1998 enhance virus replication in mammalian cells. *J Virol* **81**:8112-8121.
28. **Gack MU, Albrecht RA, Urano T, Inn KS, Huang IC, Carnero E, Farzan M, Inoue S, Jung JU, Garcia-Sastre A.** 2009. Influenza A virus NS1 targets the ubiquitin ligase TRIM25 to evade recognition by the host viral RNA sensor RIG-I. *Cell Host Microbe* **5**:439-449.
29. **Marazzi I, Ho JS, Kim J, Manicassamy B, Dewell S, Albrecht RA, Seibert CW, Schaefer U, Jeffrey KL, Prinjha RK, Lee K, Garcia-Sastre A, Roeder RG, Tarakhovsky A.** 2012. Suppression of the antiviral response by an influenza histone mimic. *Nature* **483**:428-433.
30. **Kuo RL, Zhao C, Malur M, Krug RM.** 2010. Influenza A virus strains that circulate in humans differ in the ability of their NS1 proteins to block the activation of IRF3 and interferon-beta transcription. *Virology* **408**:146-158.
31. **Noah DL, Twu KY, Krug RM.** 2003. Cellular antiviral responses against influenza A virus are countered at the posttranscriptional level by the viral NS1A protein via its binding to a cellular protein required for the 3' end processing of cellular pre-mRNAs. *Virology* **307**:386-395.
32. **Turkington HL, Juozapaitis M, Kerry PS, Aydillo T, Ayllon J, Garcia-Sastre A, Schwemmle M, Hale BG.** 2015. Novel Bat Influenza Virus NS1 Proteins Bind Double-Stranded RNA and Antagonize Host Innate Immunity. *J Virol* **89**:10696-10701.
33. **Zhao X, Tefsen B, Li Y, Qi J, Lu G, Shi Y, Yan J, Xiao H, Gao GF.** 2016. The NS1 gene from bat-derived influenza-like virus H17N10 can be rescued in influenza A PR8 backbone. *J Gen Virol* **97**:1797-1806.
34. **Hale BG, Barclay WS, Randall RE, Russell RJ.** 2008. Structure of an avian influenza A virus NS1 protein effector domain. *Virology* **378**:1-5.

- 615 35. **Kerry PS, Ayllon J, Taylor MA, Hass C, Lewis A, Garcia-Sastre A, Randall RE,**
616 **Hale BG, Russell RJ.** 2011. A transient homotypic interaction model for the influenza
617 A virus NS1 protein effector domain. *PLoS One* **6**:e17946.
- 618 36. **Ayllon J, Russell RJ, Garcia-Sastre A, Hale BG.** 2012. Contribution of NS1
619 effector domain dimerization to influenza A virus replication and virulence. *J Virol*
620 **86**:13095-13098.
- 621 37. **Aramini JM, Ma LC, Zhou L, Schauder CM, Hamilton K, Amer BR, Mack TR,**
622 **Lee HW, Ciccocanti CT, Zhao L, Xiao R, Krug RM, Montelione GT.** 2011. Dimer
623 interface of the effector domain of non-structural protein 1 from influenza A virus: an
624 interface with multiple functions. *J Biol Chem* **286**:26050-26060.
- 625 38. **Hale BG, Jackson D, Chen YH, Lamb RA, Randall RE.** 2006. Influenza A virus
626 NS1 protein binds p85beta and activates phosphatidylinositol-3-kinase signaling. *Proc*
627 *Natl Acad Sci U S A* **103**:14194-14199.
- 628 39. **Hale BG, Batty IH, Downes CP, Randall RE.** 2008. Binding of influenza A virus
629 NS1 protein to the inter-SH2 domain of p85 suggests a novel mechanism for
630 phosphoinositide 3-kinase activation. *J Biol Chem* **283**:1372-1380.
- 631 40. **Fan S, Macken CA, Li C, Ozawa M, Goto H, Iswahyudi NF, Nidom CA, Chen H,**
632 **Neumann G, Kawaoka Y.** 2013. Synergistic effect of the PDZ and p85beta-binding
633 domains of the NS1 protein on virulence of an avian H5N1 influenza A virus. *J Virol*
634 **87**:4861-4871.
- 635 41. **Hale BG, Kerry PS, Jackson D, Precious BL, Gray A, Killip MJ, Randall RE,**
636 **Russell RJ.** 2010. Structural insights into phosphoinositide 3-kinase activation by the
637 influenza A virus NS1 protein. *Proc Natl Acad Sci U S A* **107**:1954-1959.
- 638 42. **Pichlmair A, Kandasamy K, Alvisi G, Mulhern O, Sacco R, Habjan M, Binder**
639 **M, Stefanovic A, Eberle CA, Goncalves A, Burckstummer T, Muller AC, Fauster**
640 **A, Holze C, Lindsten K, Goodbourn S, Kochs G, Weber F, Bartenschlager R,**
641 **Bowie AG, Bennett KL, Colinge J, Superti-Furga G.** 2012. Viral immune
642 modulators perturb the human molecular network by common and unique strategies.
643 *Nature* **487**:486-490.
- 644 43. **Ayllon J, Hale BG, Garcia-Sastre A.** 2012. Strain-specific contribution of NS1-
645 activated phosphoinositide 3-kinase signaling to influenza A virus replication and
646 virulence. *J Virol* **86**:5366-5370.
- 647 44. **Hrincius ER, Hennecke AK, Gensler L, Nordhoff C, Anhlan D, Vogel P,**
648 **McCullers JA, Ludwig S, Ehrhardt C.** 2012. A single point mutation (Y89F) within
649 the non-structural protein 1 of influenza A viruses limits epithelial cell tropism and
650 virulence in mice. *Am J Pathol* **180**:2361-2374.
- 651 45. **Ehrhardt C, Wolff T, Ludwig S.** 2007. Activation of phosphatidylinositol 3-kinase
652 signaling by the nonstructural NS1 protein is not conserved among type A and B
653 influenza viruses. *J Virol* **81**:12097-12100.

- 654 46. **Patzina C, Botting CH, Garcia-Sastre A, Randall RE, Hale BG.** 2017. Human
655 interactome of the influenza B virus NS1 protein. *J Gen Virol* **98**:2267-2273.
- 656 47. **Lopes AM, Domingues P, Zell R, Hale BG.** 2017. Structure-Guided Functional
657 Annotation of the Influenza A Virus NS1 Protein Reveals Dynamic Evolution of the
658 p85beta-Binding Site During Circulation in Humans. *J Virol* doi:10.1128/JVI.01081-
659 17.
- 660 48. **Li W, Wang G, Zhang H, Shen Y, Dai J, Wu L, Zhou J, Jiang Z, Li K.** 2012.
661 Inability of NS1 protein from an H5N1 influenza virus to activate PI3K/Akt signaling
662 pathway correlates to the enhanced virus replication upon PI3K inhibition. *Vet Res*
663 **43**:36.
- 664 49. **Shen YY, Liang L, Zhu ZH, Zhou WP, Irwin DM, Zhang YP.** 2010. Adaptive
665 evolution of energy metabolism genes and the origin of flight in bats. *Proc Natl Acad*
666 *Sci U S A* **107**:8666-8671.
- 667 50. **Seim I, Fang X, Xiong Z, Lobanov AV, Huang Z, Ma S, Feng Y, Turanov AA,**
668 **Zhu Y, Lenz TL, Gerashchenko MV, Fan D, Hee Yim S, Yao X, Jordan D, Xiong**
669 **Y, Ma Y, Lyapunov AN, Chen G, Kulakova OI, Sun Y, Lee SG, Bronson RT,**
670 **Moskalev AA, Sunyaev SR, Zhang G, Krogh A, Wang J, Gladyshev VN.** 2013.
671 Genome analysis reveals insights into physiology and longevity of the Brandt's bat
672 *Myotis brandtii*. *Nat Commun* **4**:2212.
- 673 51. **Zhang G, Cowled C, Shi Z, Huang Z, Bishop-Lilly KA, Fang X, Wynne JW,**
674 **Xiong Z, Baker ML, Zhao W, Tachedjian M, Zhu Y, Zhou P, Jiang X, Ng J,**
675 **Yang L, Wu L, Xiao J, Feng Y, Chen Y, Sun X, Zhang Y, Marsh GA, Crameri G,**
676 **Broder CC, Frey KG, Wang LF, Wang J.** 2013. Comparative analysis of bat
677 genomes provides insight into the evolution of flight and immunity. *Science* **339**:456-
678 460.
- 679 52. **Campa CC, Ciruolo E, Ghigo A, Germina G, Hirsch E.** 2015. Crossroads of PI3K
680 and Rac pathways. *Small GTPases* **6**:71-80.
- 681 53. **Fruman DA, Chiu H, Hopkins BD, Bagrodia S, Cantley LC, Abraham RT.** 2017.
682 The PI3K Pathway in Human Disease. *Cell* **170**:605-635.
- 683 54. **Biesold SE, Ritz D, Gloza-Rausch F, Wollny R, Drexler JF, Corman VM, Kalko**
684 **EK, Oppong S, Drosten C, Muller MA.** 2011. Type I interferon reaction to viral
685 infection in interferon-competent, immortalized cell lines from the African fruit bat
686 *Eidolon helvum*. *PLoS One* **6**:e28131.
- 687 55. **Eckerle I, Ehlen L, Kallies R, Wollny R, Corman VM, Cottontail VM, Tschapka**
688 **M, Oppong S, Drosten C, Muller MA.** 2014. Bat airway epithelial cells: a novel tool
689 for the study of zoonotic viruses. *PLoS One* **9**:e84679.
- 690 56. **Reuther P, Gopfert K, Dudek AH, Heiner M, Herold S, Schwemmle M.** 2015.
691 Generation of a variety of stable Influenza A reporter viruses by genetic engineering
692 of the NS gene segment. *Sci Rep* **5**:11346.

- 693 57. **Solorzano A, Webby RJ, Lager KM, Janke BH, Garcia-Sastre A, Richt JA.** 2005.
694 Mutations in the NS1 protein of swine influenza virus impair anti-interferon activity
695 and confer attenuation in pigs. *J Virol* **79**:7535-7543.
- 696 58. **Anonymous.** The PyMOL Molecular Graphics System. Version 18 Schroedinger,
697 LLC.
- 698
- 699

Figure 1

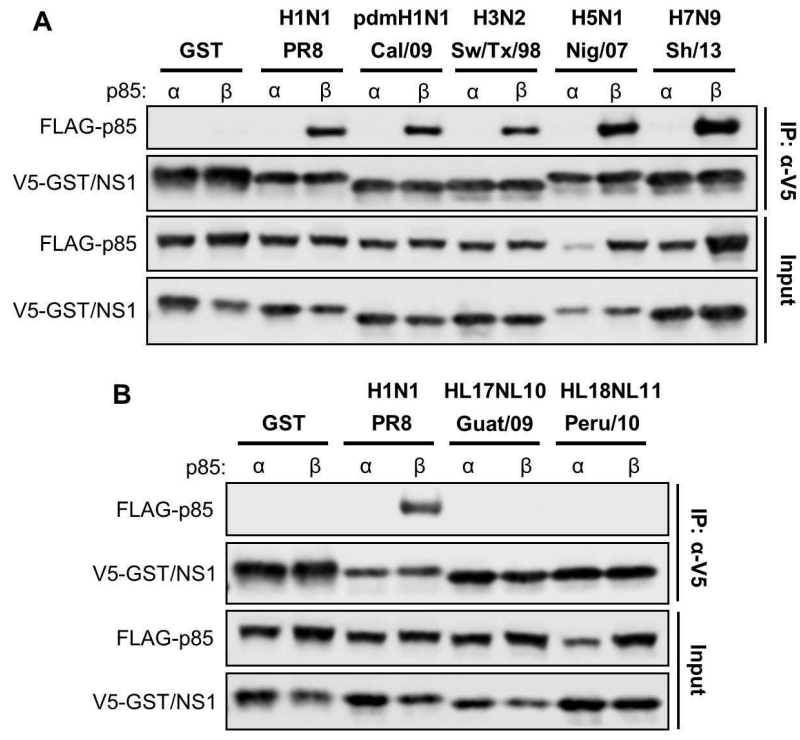


Figure 2

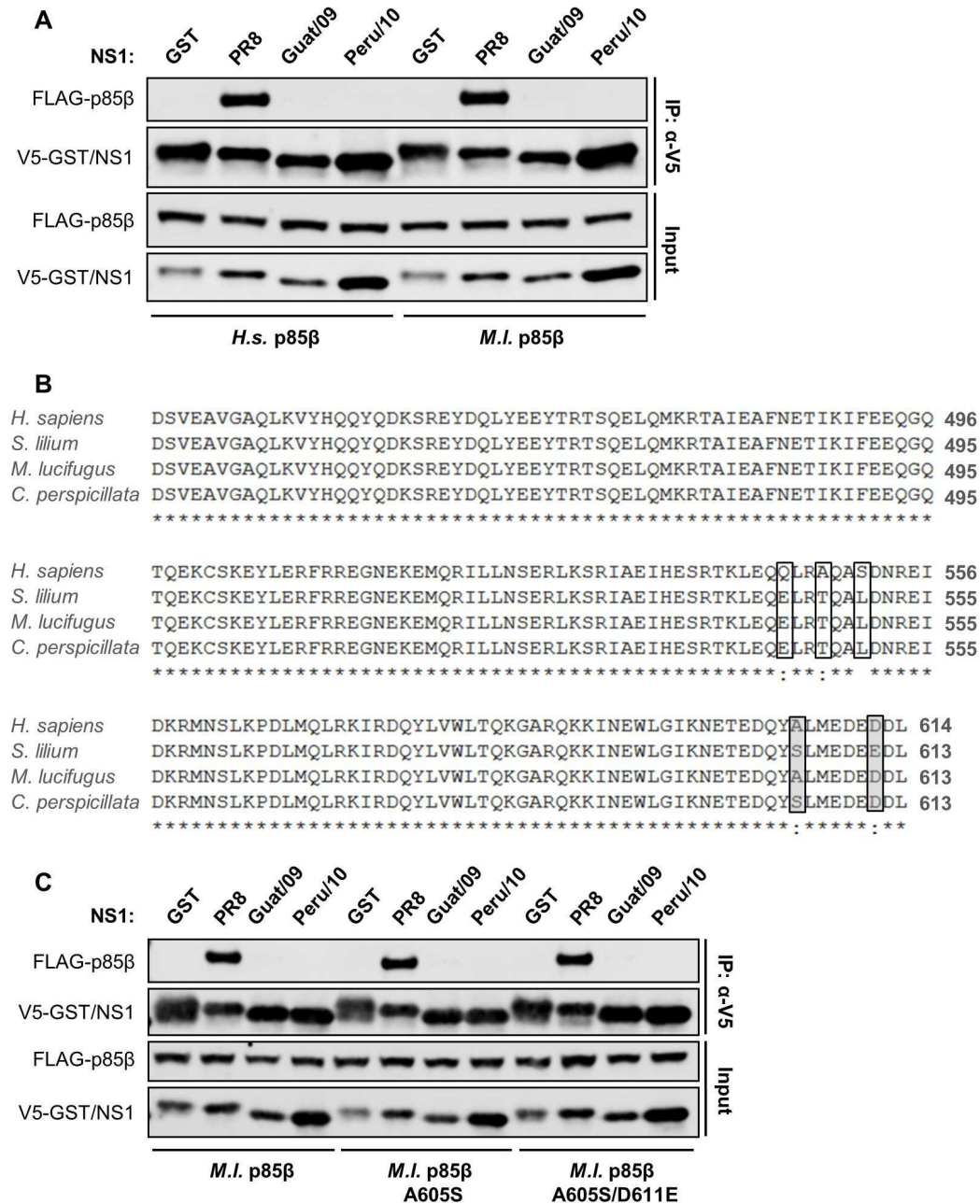


Figure 3

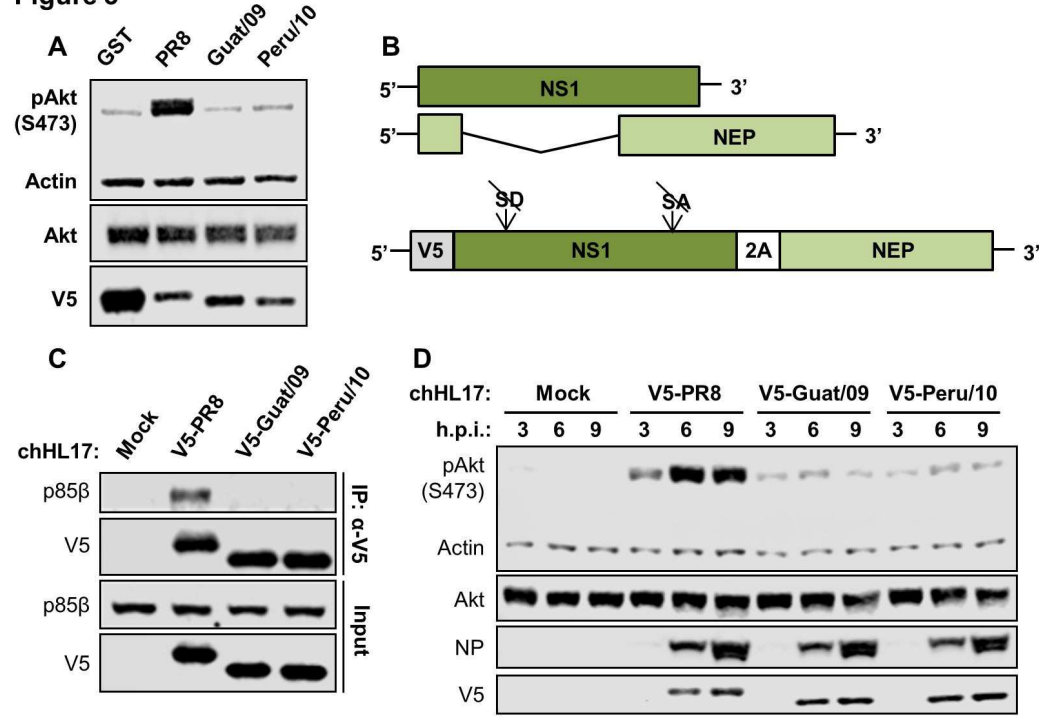


Figure 4

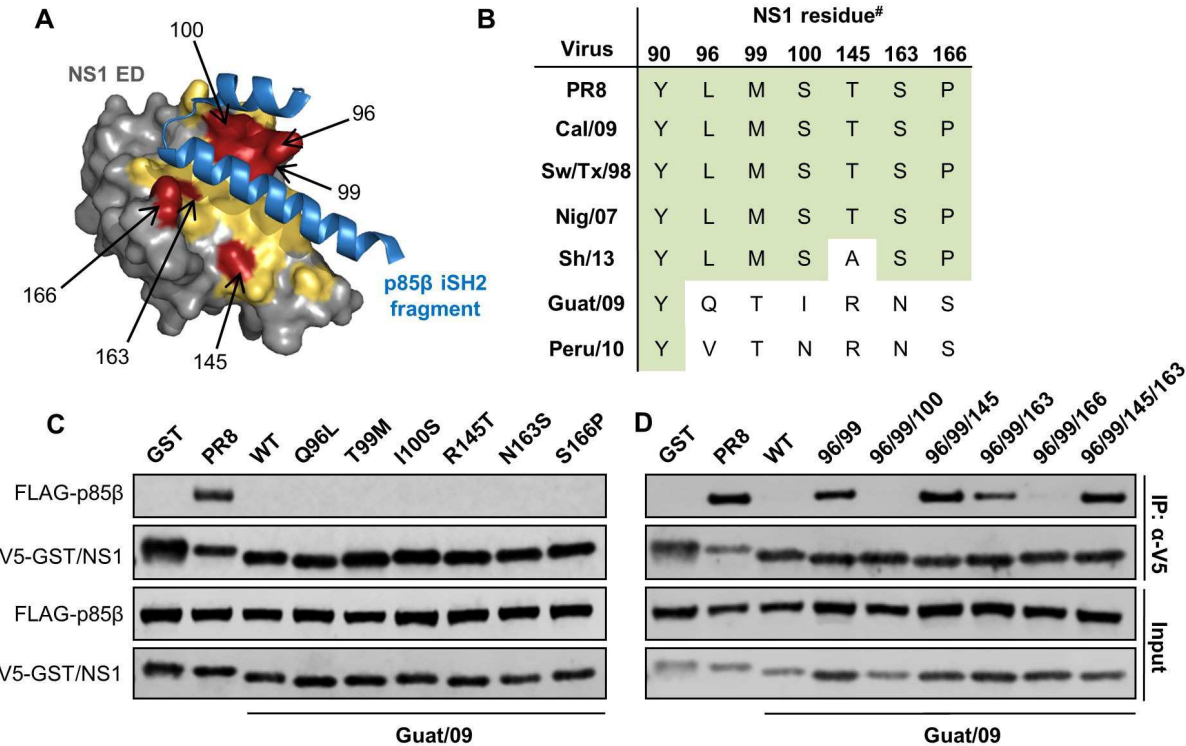


Figure 5

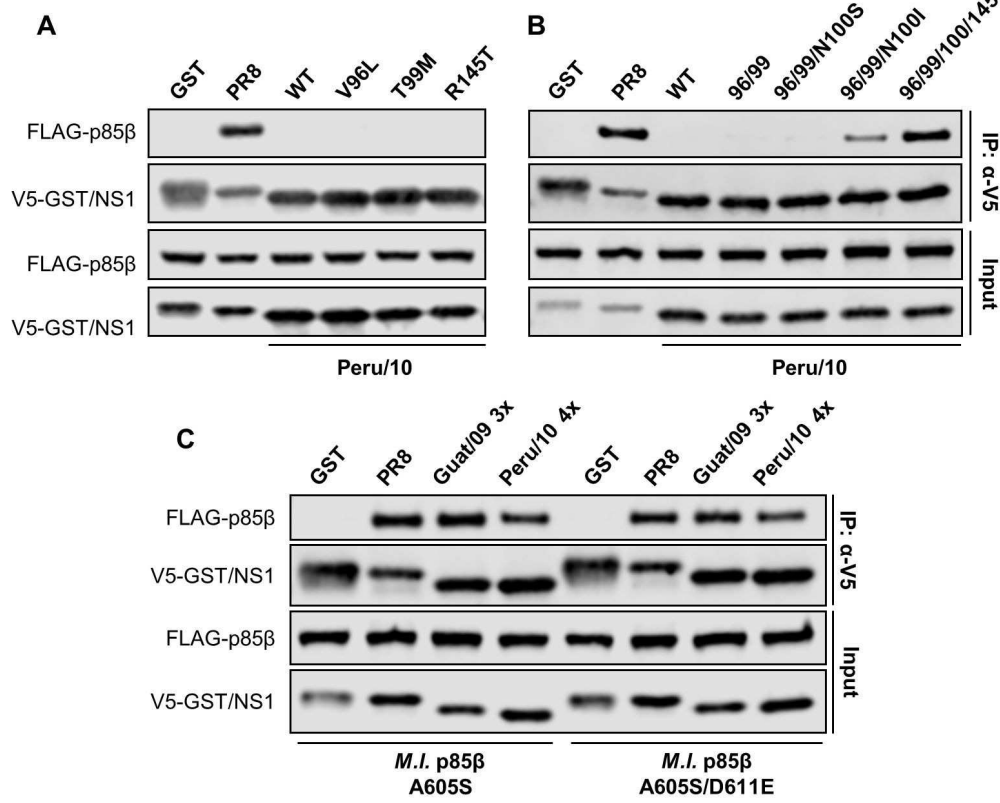


Figure 6

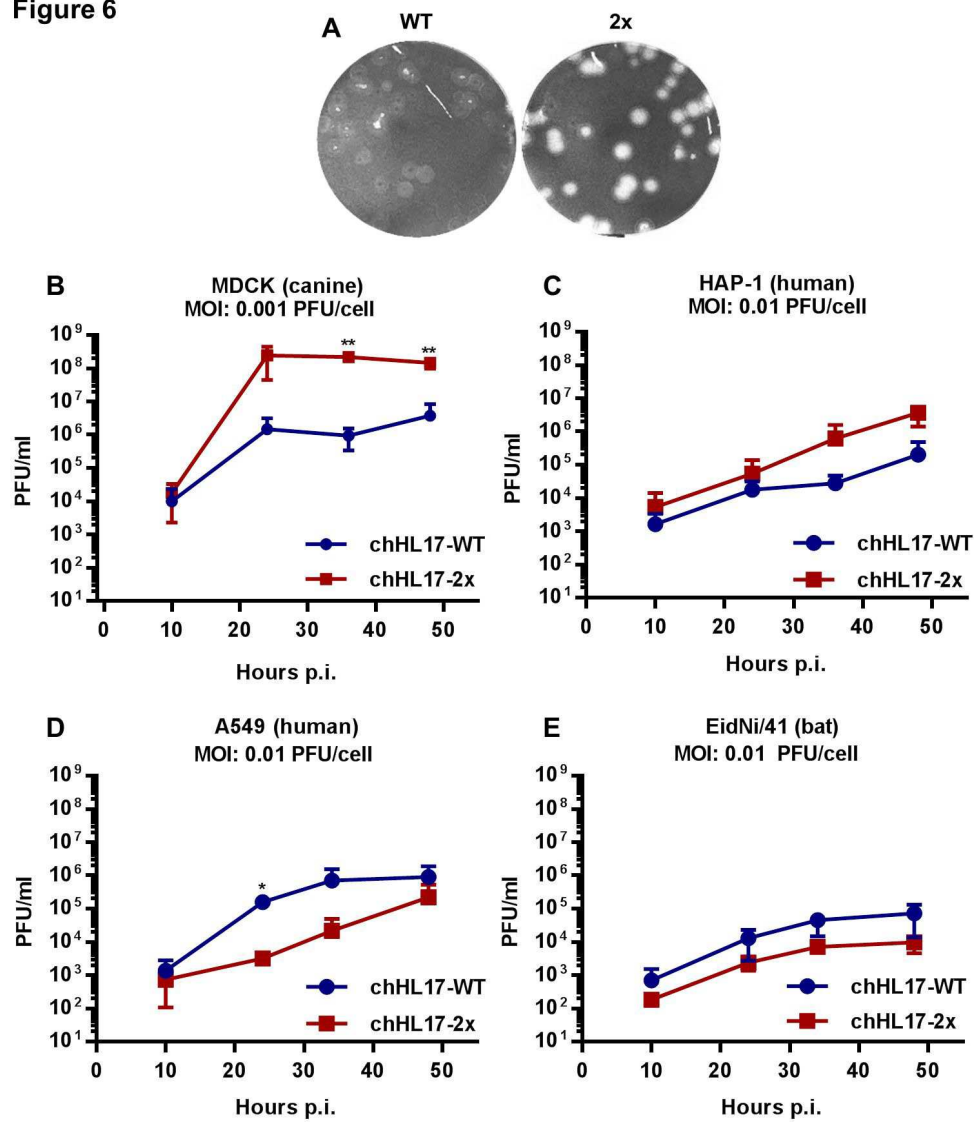


Figure 7

